MAGIC Major Atmospheric Gamma Imaging Cerenkov Telescope

MAGIC-TDAS 06-08

The Crab Nebula in VHE–γ–rays from 60GeV to 9TeV

N. Otte, P. Majumdar

<otte@mppmu.mpg.de>,<pratik@mppmu.mpg.de>

July 17, 2006

Abstract

We present the analysis of MAGIC data from the Crab nebula. Our purpose was to test the standard analysis chain starting from the calibration up to the derivation of an unfolded spectrum. We also derive a spectrum from the Crab nebula between 60GeV and 9TeV that is reflecting our latest understanding of the performance of the telescope. The analyzed data comprises about 20hours of data that was taken at Zenith angles $< 30°$ between October and December 2005. We quantified our systematic uncertainties in the analysis by processing the same calibrated data sample with two different image cleaning methods and different cuts applied in the analysis.

The integrated sensitivity > 200 GeV obtained from our analysis is 2.2% in units of the Flux from the Crab nebula after 50 hours of observation.

Contents

1 Introduction

The Crab nebula is per definition the "standard candle" in VHE $\gamma-$ ray experiments. Up to now no variability in the flux of $\gamma-$ rays from Crab has been reported above a few hundred GeV up to several tens of TeV of energies. Thus the Crab nebula provides us with good means to study and understand the telescope performance.

In this note we describe the analysis of a large data sample (20 hours) of the Crab nebula in an energy range between 50 GeV and 5 TeV. The data has been recorded at Zenith angles below 30° in the second half of the year 2005 between October and December. Such a large data sample allows to measure the Crab spectrum with high precision down to 100 GeV. At the same time one can quantify the systematic uncertainties in the analysis below 100 GeV if only standard tools are used. At higher energies the signal to background ratio is such that a good comparison between Monte Carlo Simulations and Data can be performed.

This note is organized as follows. In the first part the selection of the data is discussed as well as a short overview of the methods is given that have been used for the processing of the data up to the calculation of image parameters and gamma/hadron separation. Apart from the standard image cleaning we have also used an image cleaning procedure that is including the time information of each pixel. This "time image cleaning" is discussed in more detail as it has not been presented elsewhere. In the second and main part of the note we present and discuss results of the analysis. This includes:

- spectra of the nebula obtained with different cleanings and analysis cuts
- sky maps
- integrated and differential sensitivities
- Comparison with other experimental data
- Comparison of Monte Carlo simulations with data

2 Data processing

The processing of the data has been done in the following steps:

2.1 Selection of the Data Set

The selection of a sub sample out of the full data sample is primarily driven by an as low as possible analysis threshold. As the trigger threshold of the telescope E_{thresh} strongly depends on the Zenith angle of the observation

$$E_{\mathrm{thresh}} \propto \frac{1}{\cos^2\theta} \quad .$$

For our analysis we accepted only runs that were taken at Zenith angles below 30°. This is equivalent to a maximum allowed increase of the trigger threshold of 30%. We analyzed only data that was taken by directly pointing to the Crab Nebula. In this mode the majority of the observations of the Crab Nebula was carried out in 2005. Another additional criterium for selection was that the moon was below horizon during data taking. This is especially important when analyzing events below 100 GeV as otherwise the events would suffer from contamination by moonlight. Wherever available we excluded runs based on comments in the runbook that indicate technical problems with the telescope or bad weather reported by the shifters.

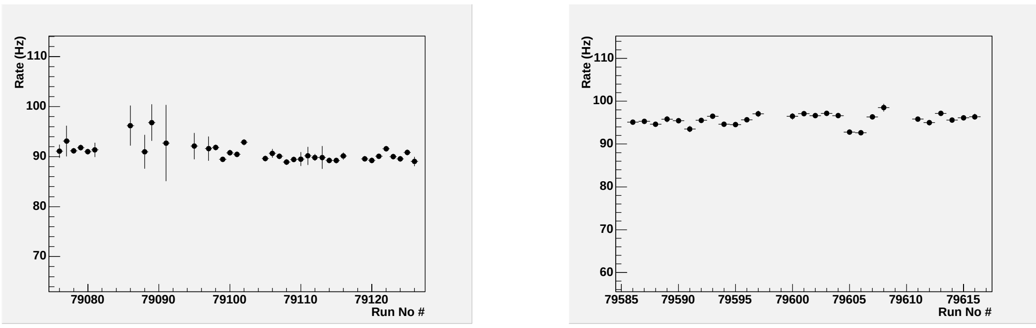

Figure 1: *Left panel*: The trigger rate averaged per run after 10/5 image cleaning and application of filter cuts for Crab on a particular night. *Right panel*: The trigger rate for the Off data (OffCrab13).

Runs that survived all above mentioned selection criteria had been calibrated as will be explained in next section. After calibration and calculation of image parameters the rate dependence vs. time was checked on a day by day basis. Runs that showed fluctuations or too low/high trigger rates were rejected from further analysis. Figure 1 shows the trigger rates after image cleaning and application of filter cuts for ON and OFF data for particular nights of observation. It is seen that the rates are reasonably steady and similar in both the cases.

In Table 1 we have listed the days that survived all selection criteria. The total observation time of the sub sample amounts to 18 hours if a Zenith angle cut of $< 20°$ is applied. If the Zenith angle is loosened to $< 30°$ the observation time increases to 20 hours.

Table 1: Data selected for analysis below 20° Zenith angle.

Date	**Rates** [Hz]	**On Time** [min]	**Zd–Range** [°]
05.10.2005	220	90	$7 \ldots 23$
12.10.2005	170	80	$7 \ldots 19$
28.10.2005	180	170	$7 \ldots 23$
29.10.2005	160	90	$8 \ldots 20$
05.11.2005	150	60	$7 \ldots 20$
10.11.2005	130	60	$7 \ldots 20$
03.12.2005	140	60	$7 \ldots 11$
05.12.2005	140	60	$7 \ldots 10$
07.12.2005	140	50	$7 \ldots 10$
09.12.2005	150	50	$7 \ldots 14$
23.12.2005	130	50	$7 \ldots 13$
25.12.2005	130	60	$7 \ldots 13$
27.12.2005	140	100	$7 \ldots 14$
31.12.2005	120	100	$7 \ldots 15$
total: 1080 min			

We applied the same selection criteria to off data that was used to determine the background. To increase the statistics of the OFF data sample we also used, apart from the dedicated OFF Crab data, off data taken on the extragalactic OffMrk501–2 position. In total, about 9 hours of OFF data were used in this analysis. It should be noted that the background runs for the two different analysis (standard image cleaning and time image cleaning) were different.

2.2 Calibration

For calibration i.e. determination of conversion factors from ADC counts to photoelectrons we applied the F-factor method which is the defacto standard method. For extraction of the signal from the data we used the Digital filter method with pulse position check switched off. This was necessary due to a known dependence of the delay in the trigger logic on the position of the event in the camera.

2.3 Image Cleaning

Before the calculation of image parameters a cleaning method is applied that is rejecting pixels in a shower image that only contain noise. In the standard cleaning procedure the number of photo electrons in a pixel is the only information that is used as a criterium to decide if a pixel contains a useful signal or not.

2.3.1 Standard Cleaning

The algorithm of the standard cleaning procedure is following three steps.

1. All pixels with a signal content above a predefined level (CleanLvl1) are recognized as core pixel
2. Out of the multitude of selected pixels those that do not have a core pixel as direct neighbor are discarded
3. In the direct vicinity of the remaining clusters of core pixels the algorithm searches for boundary pixels in the last cleaning step. To be selected as boundary pixel the candidate has to meet two requirements. First it has to have a signal above a predefined threshold (CleanLvl2) and second the pixel has to have a direct next neighbor already selected in a previous step

The last step of the cleaning procedure can be repeated several times.

2.3.2 Image Cleaning using Time

The standard cleaning procedure described above is very effective in rejecting noise if the levels for core and boundary cut are sufficiently high above the noise level. For large images (energies >100 GeV) this is not a problem. At lower energies high cleaning cuts will result in significant losses of the shower image. By lowering the cleaning levels to retain the shower image one has to pay the price of picking up pixels that only have a signal coming from the Night Sky background or electronic noise. The image becomes distorted. The situation can be improved by requiring as additional constraint a coincidence in the arrival time of the signal between adjacent pixels. In this way most of the pixels that only have a signal coming from the Night Sky Background are rejected.

We have used a time cleaning (Mars class MImageCleanTime) that is making use of this coincidence requirement. The implementation is similar to the one proposed by the Berlin group. A major difference to the Berlin method is that the applied procedure only needs calibrated data. In the following we describe the algorithm in more detail. For illustrative purposes the float chart is displayed in Figure 2.

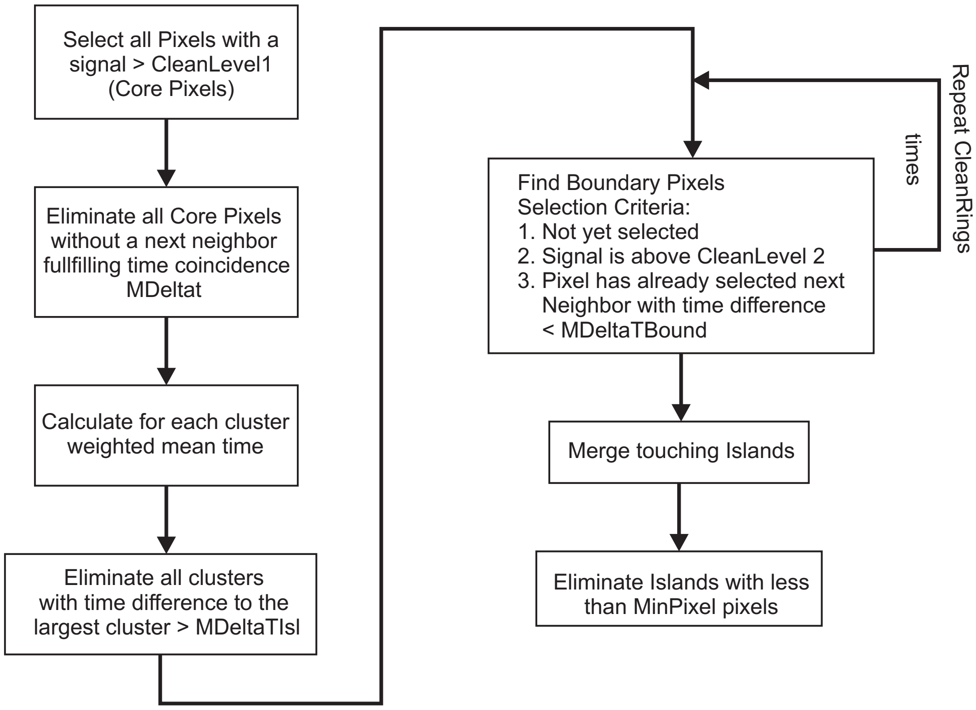

Figure 2: Flow chart of the time image cleaning procedure used in some of the analysis. See text for explanation.

1. Selection of all pixels with a signal content larger than defined by *CleanLevel1*

2. For each of these pixels it is searched among all adjacent pixels for at least one next neighbor that fulfills two conditions. First the pixel has been selected in the first step and second the difference in arrival times between the two pixels is less than a predefined value (typical 1-2 FADC slices).

   If no such adjacent pixel can be found the pixel is rejected and otherwise selected as one of the core pixels.

3. All touching core pixels (next neighbors) are grouped in clusters. For each cluster the average arrival time of all signals is calculated. To calculate the average arrival time the individual arrival times are weighted with the signal.

4. The clusters are sorted according to their size and the difference of the weighted mean time for each cluster to the largest cluster is calculated. If the absolute difference is too large the cluster is being rejected.

5. The selection of boundary pixels proceeds in a similar way as for the core pixels. Beside the requirement of a minimal signal content a boundary pixel has also to be close in time to an adjacent pixel. This step can be iterated more than once.

6. In the next step all clusters are merged that are touching each other. Finally all clusters that do not fulfill the requirement of a minimum number of pixels are rejected.

Comparison of Time Image Cleaning with standard Cleaning In Figure 3 the reconstructed charge distribution of different image cleanings are plotted for true energies between 75 and 100 GeV. The blue distribution is for time image cleaning with absolute cuts for core and boundary pixels of 5 and 1. On average 90% of the charge of the event is reconstructed. The tail extending towards and beyond unity in terms of relative reconstructed signal is due to noise pickup. If the same cleaning levels are applied without the time coincidence requirement much more noise is being picked up (right red curve is shifted to the right). The left distributions is for standard cleaning with levels of 7 and 5 photoelectrons. It shows that on average 50% of the signal of each event is lost. The three distributions indicate that by using the time information from each pixel most of the shower is reconstructed without integrating too much noise.

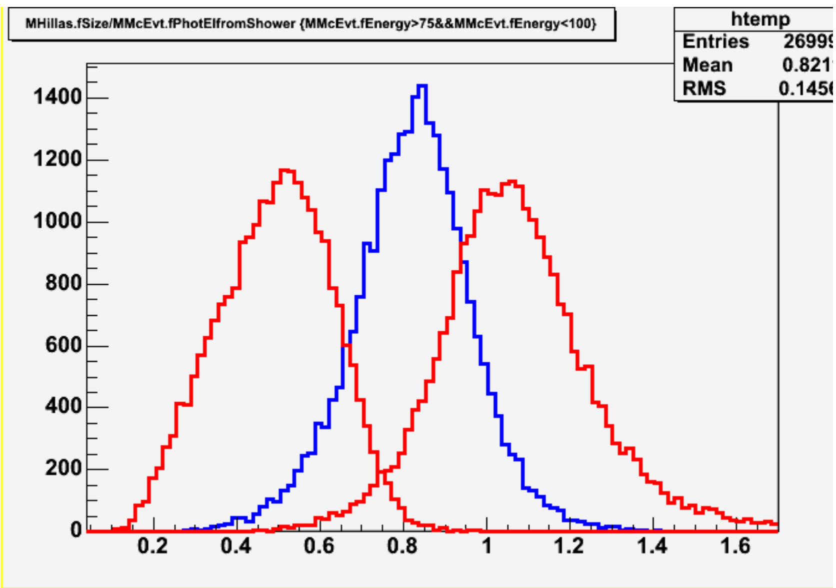

Figure 3: Relative fraction of reconstructed size per event, MC–gamma events. The red curves represent standard cleanings. For the left distribution 7 photoelectrons as core and 5 photoelectrons as boundary cut has been applied. For the left distribution cuts of 5 and 1 photoelectrons were applied. The blue distribution has been processed with time image cleaning 5 and 1 photoelectrons. See text for discussion.

2.3.3 Applied Cleaning Levels

Cleaning of the calibrated events was performed using three different sets of cleaning levels.

- absolute 5 phe core 1 phe boundary using time image cleaning
- absolute 5 phe core 3 phe boundary using time image cleaning
- absolute 6 phe core 4 phe boundary using time image cleaning
- absolute 10phe core 5phe boundary using standard cleaning
- absolute 7phe core 5phe boundary using standard cleaning
- scaled 4σ core 3σ boundary using standard cleaning

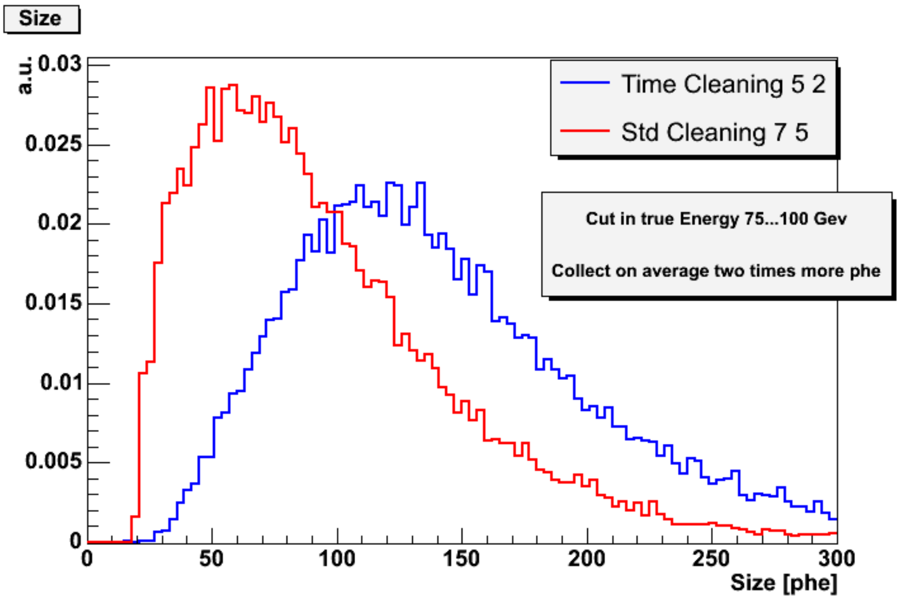

Figure 4: Size distribution of two MC–data sample processed with two different image cleanings; red standard cleaning 7 and 5 photoelectrons, blue time cleanig 5 and 1 photoelectron

For the set of image cleanings in which a core pixel cut of 5 phe is applied the time coincidence window was set to ± 2 FADC slices whereas for the cleaning with a 6 phe core pixel cut the coincidence window was set to ± 1 FADC slice.

After cleaning of the events a standard second moment analysis has been applied to the data (calculation of Hillas parameters).

2.4 Gamma Hadron Separation

A pre-defined set of filter cuts were applied to the data before the classification of events. These cuts included a corepixel cut, leakage cut and spark cuts. For the separation of gammas and hadrons we applied the RandomForest method. As hadron training sample the OffCrab-13 data taken on January 2nd 2006 were used. The MC gammas were simulated using a global PSF of $\sigma = 0.052°$. (by adding a PSF of 14 mm in X and Y directions at the camera simulation level) . The training of RF was done using the standard MC production. (1/3 rd for gamma hadron separation, 1/3 rd for energy estimation and the rest as test sample). In addition a large sample of High Energy MC gammas were also used as the test sample to compute the collection area, cut efficiencies etc.

In this note we present the results from the traditional Alpha analysis, however a DISP analysis was also performed to obtain the Skymaps.

The training of the random forest was done by using the following Hillas parameters:

- Size
- Dist
- Width
- Length

In addition to the standard Hillas parameters the parameters Conc5 and Conc7 were also used as well as the Asymmetry parameter

$$\frac{\mathrm{M3Long} \times \mathrm{CosDeltaAlpha}}{|\mathrm{CosDeltaAlpha}|}$$

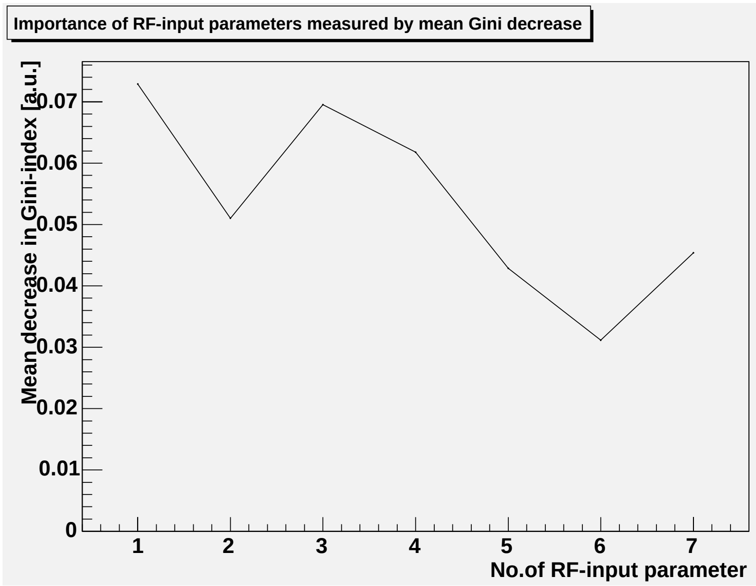

Figure 5: Gini index for time image cleaning 6 4. Parameters from left to right are size, dist, width, length, conc5, conc7 and an asymmetry parameter

Figure 5 shows the weights which are put to the different parameters for training (gini index).

2.5 Energy Estimation

The energy estimation of the events was also carried out by applying the random forest method to Monte Carlo gammas. Image Parameters used in the energy estimation are:

- Size
- Dist
- Width
- Length
- Conc
- Conc5
- Leakage
- Zenith angle
- $\log \mathrm{Size}/(\mathrm{Length} \times \mathrm{Width}$
- Gamma Energy

3 Results

3.1 Sensitivity

The steady TeV emission that is originating from the Crab Nebula serves as our "standard candle". The sensitivity of the telescope can be tested on the Crab nebula and compared to other experiments and expectations from Monte Carlo simulations. If the sensitivity stays constant over the whole period of data taking it can be concluded that the telescope is operating stable.

On the other hand one can argue that the calculation of the sensitivity is providing useful insight into the quality of the data.

For the above stated reasons we have calculated out of the pre selected data sample that is summarized in Table 1 the sensitivity of MAGIC.

We first trained our cuts for optimal significance on the Crab data from 05.10.2005 and verified them on the data from the 31.12.2005 and on the whole data sample. All tests gave the following cuts for highest significance that have been applied for all sensitivity measurements:

- $0.4° <$ Distance $< 1.1°$
- Size>400 phe
- Alpha$< 7.5°$
- Hadronness< 0.10
- Number of islands $= 1$
- Number of core pixels > 5

The peak in the energy distribution of MC–Gamma events yields a threshold of 200GeV for these cuts. [1]

3.1.1 Integrated Sensitivity >200GeV

Applying the above cuts to the whole data sample of 18 hours result in the alpha distribution of Figure 6. The significance of the signal derived by extrapolation of the background and calculated following Li&Ma formula 17 is 81.66 σ. This results in an integrated sensitivity above 200 GeV of 17.6 $\sigma/\sqrt{\mathrm{hr}}$ for γ–emission from the Crab Nebula.

Another figure that is commonly used to compare different experiments is the minimum flux in units of the flux from the Crab Nebula needed for a significant (5 σ) detection after 50 hours of observation. For this figure of merit the following definition of the significance S is used

$$S = \frac{N_{\mathrm{Excess}}}{\sqrt{N_{\mathrm{Background}}}} \quad .$$

If applied to Figure 6 the result is a minimum flux level of 2.3% that is required from a source with a Crab like spectrum to give a 5 σ signal after 50 hours of observation. We also derived the sensitivity by using off data to estimate the background and obtained a consistent sensitivity of 2.4 % Crab in 50 hours of observation.

[1] These cuts are for time image cleaning method and comparable results were obtained from the standard image cleaning analysis, as shown in a table

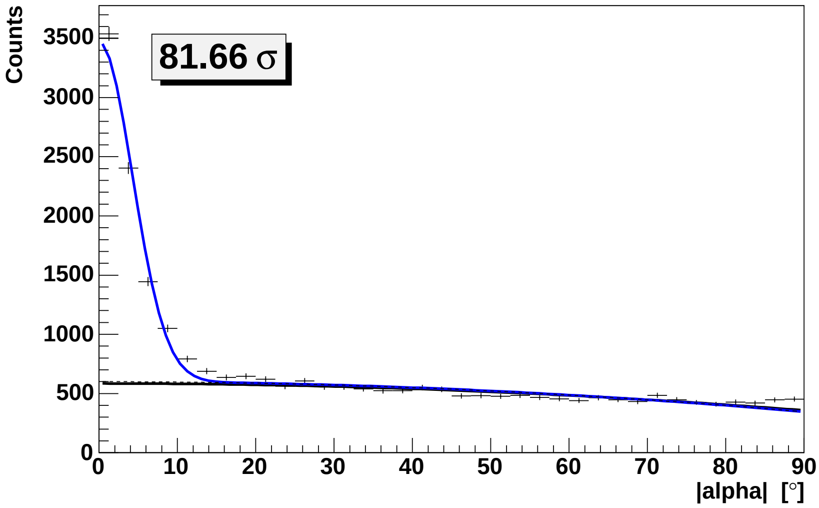

Figure 6: Alpha Plot of the total Crab data set (18 hrs). On events ($|\alpha| < 7.5°$): 7300, OFF events from fit: 1800, Excess: 5500

Apart from deriving the sensitivity out of the whole data sample it is instructive for the earlier mentioned reasons to calculate the sensitivity on a day by day basis. This is possible as a one hour observation of the Crab nebula with the MAGIC telescope results in a sufficiently strong signal. The results of this study are listed in Table 2. The average values off all individual days are consistent within errors with the values derived from the full data set. The root mean square of the distributions are quoted in the last row of Table 2. They indicate day by day fluctuations on the level of 10% and stability of the telescope for the period of time that has been analyzed.

3.1.2 Differential Sensitivity

The integrated sensitivity was derived with an analysis threshold of 200 GeV. When applying this threshold we obtained the highest significance. A lower analysis threshold would reduce the significance of the signal because of the background. A higher analysis threshold would also reduce the significance but because of a loss of gamma events.

We calculated the differential sensitivity i.e., the sensitivity in different bins of energy. We have done this by dividing the Energy range between 100GeV and 1TeV in six bins. The derived sensitivities and the peak energy for each bin are listed in Table 3.

Table 2: Integral Sensitivity of Crab ($>$ 200 GeV); In the last row of the table the RMS of the distributions is quoted in brackets.

	standard cleaning 10 5 absolute		**time cleaning 6 4 absolute**	
date	**Significance** $[\sigma/\sqrt{\mathrm{hr}}]$	**Sensitivity** [% Crab, 50 hrs, 5σ]	**Significance** $[\sigma/\sqrt{\mathrm{hr}}]$	**Sensitivity** [% Crab, 50 hrs, 5σ]
05.10.2005	18.1	2.11	16.3	2.3
12.10.2005	18.8	1.94	21.5	1.9
28.10.2005	18.4	2.08	15.6	2.3
29.10/2005	18.5	1.99	16.5	2.8
05.11.2005	17.5	2.28	17.7	2.4
10.11.2005	17.8	2.11	20.0	2.0
03.12.2005	17.7	2.03	20.8	2.1
05.12.2005	14.5	2.74	13.4	3.0
07.12.2005	17.8	1.97	16.6	2.3
09.12.2005	17.9	2.04	17.0	2.2
23.12.2005	15.1	2.52	15.5	2.5
25.12.2005	16.3	2.38	17.0	2.3
27.12.2005	16.4	2.29	18.0	2.2
31.12.2005	17.2	2.12	18.4	2.1
	17.3 ± 0.3 (1.3)	2.18 ± 0.06 (0.23)	17.5 ± 0.6 (2.2)	2.3 ± 0.1 (0.3)

Table 3: Sensitivity for the emission from the Crab nebula in different bins of size. The numbers marked with an asterix (*) are derived by using the full Crab data sample.

	standard cleaning 10 5 absolute all December data		**time cleaning 6 4 absolute data from 05.10.2005**	
Size bin [phe]	**Peak Energy** [GeV]	**Sensitivity** [% Crab, 50 hrs, 5σ]	**Peak Energy** [GeV]	**Sensitivity** [% Crab, 50 hrs, 5σ]
$100 \ldots 200$	90	27.8	75	35.4^{*}
$200 \ldots 400$	155	10.0	120	10.0^{*}
$400 \ldots 600$	250	6.0	220	5.8
$600 \ldots 1000$	345	4.6	320	3.5
$1000 \ldots 2000$	590	3.2	500	3.0
$2000 \ldots 5000$	1030	2.5	1000	4.0

3.2 Sky Maps

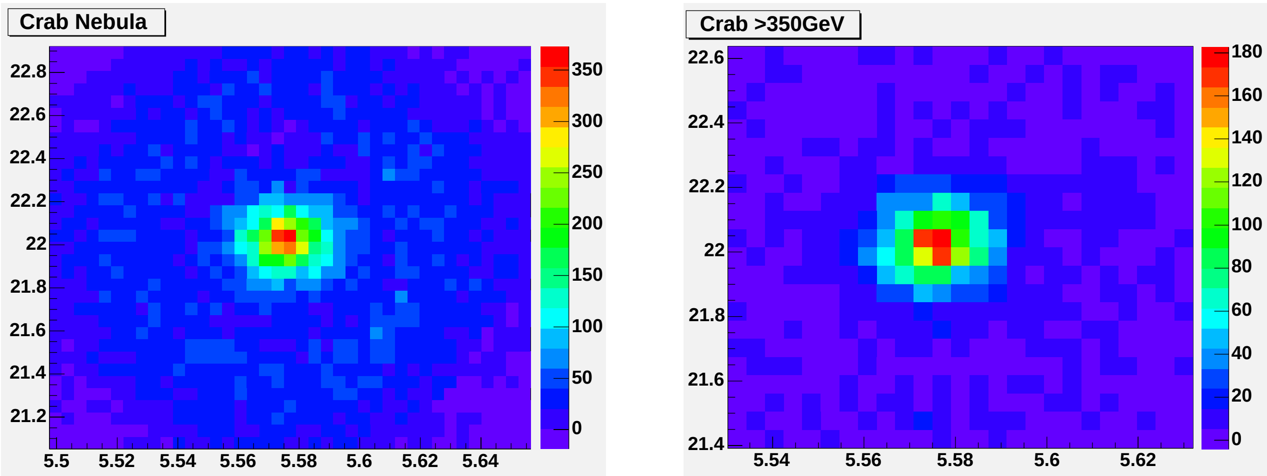

Figure 7: Sky maps produced with the Disp method. The left map includes all events with an energy >150 GeV (> 300phe). The right map includes all events with an energy > 350 GeV (>700 phe). For the maps the time image cleaning with cleaning levels 6 and 4 absolute was used.

The so called "Disp" method allows to estimate the origin of each detected γ-like event and therefore to produce sky maps which allow to study the morphology of the gamma emitting source. If the source is known to be point-like with respect to the resolution of the telescope one can study the stability of the tracking of the telescope as well as the pointing accuracy including all applied corrections.

The VHE-γ emission from the Crab nebula is known to be point-like within our resolution at least for energies above a few hundred GeV. The measured extension of the Crab nebula at these energies is therefore an indicator for the tracking/pointing accuracy of the telescope.

To produce sky maps we have processed the data with time cleaning (levels 6 4 absolute) and did not use parameters in the training of the Random Forest that included source dependent parameters. By plotting Dist/(1-Width/Length) vs. logSize we found the following parametrization for Disp

$$\mathrm{Disp} = \left(1 - \frac{\mathrm{Width}}{\mathrm{Length}}\right)\left[a - b\log Size + c\,\log^2 Size - d\,\log^3 Size + e\,\log^4 Size\right]$$

with

$$\begin{aligned} a &= 2.70003 & b &= 1.59318 \\ c &= 0.78988 & d &= 0.18358 \\ e &= 0.01703 \end{aligned}$$

Two sky maps produced with this Disp parametrization and different lower size cuts are shown in Figure 7. For the left map in the Figure a lower size cut of 300 photo electrons has been applied as well as a hadronness cut of 0.3. The right map has been compiled after a size cut of 700 photo electrons and a hadronness cut of 0.1 has been applied. The extension of the excess in the sky map for the lower size cut is significantly larger then expected from MC (cf. from Table 4: 0.1240° vs.

Table 4: From the sky maps (Figure 7) extracted source positions and extensions.

Size > [phe]	**Energy** [GeV]	**Hadr**	**Right Ascension** Mean	Sigma	**Declination** Mean	Sigma	**MC** [°]
300	150	0.3	5.5755 ± 0.0002	0.010 ± 0.0002	22.022 ± 0.002	0.124 ± 0.002	0.10
700	350	0.1	5.5760 ± 0.0002	0.0082 ± 0.0002	22.026 ± 0.002	0.095 ± 0.002	0.095
Expected Source Position:			5.5755		22.015		

0.0998°). A possible reason can e.g. be an improper estimation of the background at these energies. Other systematic effects e.g. a wrong optical PSF used in the MC or the Earth magnetic field can also give rise to the discrepancy. A possible extension of the emission region within the Crab nebula beyond the γ-pointspread funtion of the telescope can of course also not be discarded.

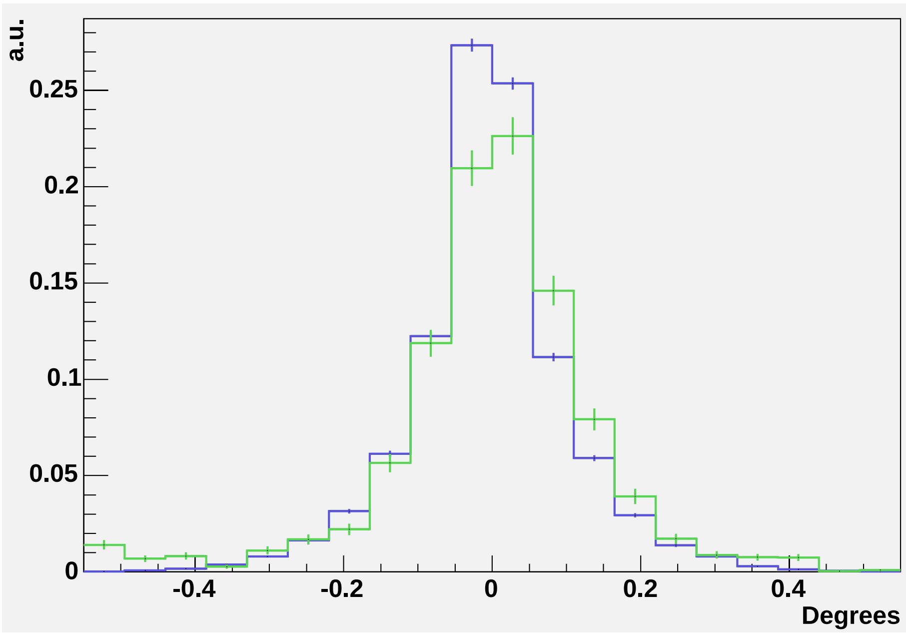

Figure 8: Point Spread Function of MC (blue) and Data (green). The PSF has been obtained from the data by cutting in the right panel of Figure 7 through the center of gravity in Right Ascension.

At larger energies the point spread function is in better agreement but not completely matching with expectations from MC (see Figure 8). The significant deviation of the position in declination from the expected position (0.024 degrees = 12 standard deviations) in both skymaps (cf. Table 4) is probably due to a systematic offset in the pointing accuracy of the telescope. The good agreement of the measured PSF with the one expected from MC at larger sizes indicates a stable tracking with an accuracy at or below the resolution of the telescope for the whole data sample. For the pointing accuracy on the other hand a systematic offset in declination of $\sim 0.01°$ can be derived from the difference between measured and expected source position.

3.3 Spectra

We computed spectra of the VHE-γ emission from the Crab nebula by using the standard Flux macro available in Mars CVS dating from April 2006.

We defined a standard set of cuts in which the hadronness and alpha cuts for different bins of energy was automatically derived from MC data. The criterium on which the cuts were derived was to retain MC gammas with an efficiency of 80% both for the alpha and hadronness cut for the data processed with the time image cleaning. For the data processed with the standard cleaning procedure the efficiencies on which the standard cuts were derived are:

- γ/hadron cut efficiency : 75%
- Dist cut efficiency : 90%
- Alpha cut efficiency : 85%

Apart from the standard cuts we also applied different cuts on the same data sets[2] to compute the spectrum. This will give us an idea of the systematics of the analysis. Here we outline the basic cuts which were changed from those derived from Monte Carlo :

A Size dependent Dist cut was applied such that it rejects events beyond the hump region as the energies of most of these events cannot be reconstructed with high accuracy. The parameterizations of the upper dist cut as defined as standard in the Flux macro is:

$$\text{Dist} < a - \exp(b - x/c) \quad | \quad \text{with } x = \text{ size in phe}$$

A set of spectra was also produced with a different upper dist cut of

$$\text{Dist} < \min(1.1^\circ + 0.4^\circ \cdot (x - 3), 1.3^\circ)\,.$$

Loosen hadronness cuts in order to achieve higher cut-efficiency and to loosen the impact of miss matches between MC and the actual data.

The 'minimum size cut' in the *flux* macro was raised from 100 photoelectrons to 250 photoelectrons and also the **cut on the number of core-pixels** was raised to 7. This was done to analyze events which are clean and well-defined. Another reason to increase the size and core-pixels cut was to become independent on the differences between the simulated and real trigger threshold of the telescope. It has also been found during MC-data comparisons of MC hadrons with *Off data* that the agreement for the number of core pixels was better for *NumCorePixels > 6.* On the other hand one has to be careful not to lower the efficiency too much below 100 GeV by applying too high cut in Size or number of core pixels.

The flux in bins of estimated energy can than be computed if the efficiency of the detector is known, i.e. the effective Collection area.

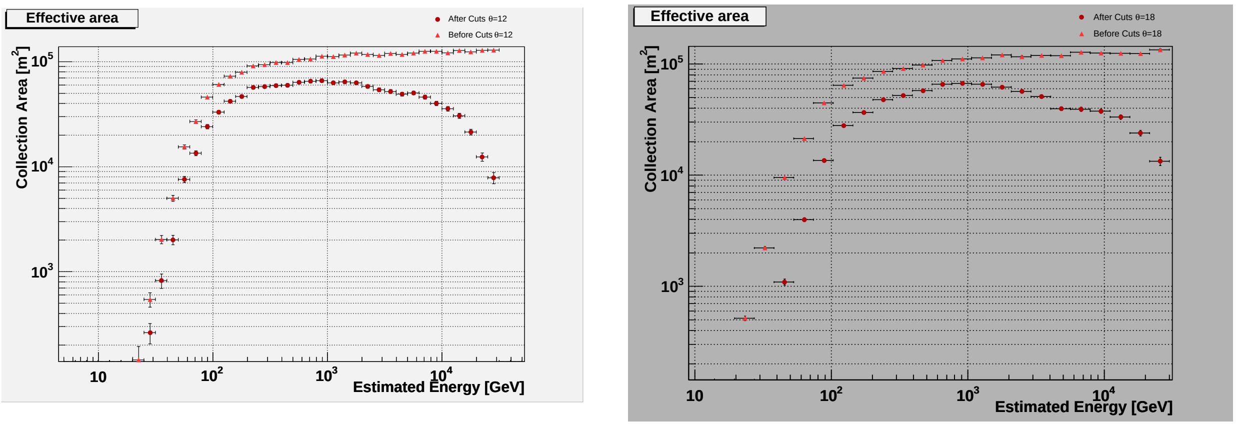

Figure 9: **Left Panel:** Collection Area before and after cuts for absolute time image cleaning of 5 and 3 applied prior to image parameter calculation. **Right Panel:** Collection Area before and after cuts for absolute standard image cleaning of 10 and 5 applied prior to image parameter calculation. The upper curve in both plots is the collection area after the trigger.

3.3.1 Collection Area

To derive the effective collection area the same cuts that have been applied to the data are applied to MC. The relative fraction of MC events that survived these cuts is then multiplied with the area in which the impact points of the simulated gammas are located. This quantity is called the collection area and computed within the Flux macro.

Figure 9 shows the collection area for two different image cleaning methods before and after cuts. The Collection area after cuts is >10,000 m^2 at 80 and 60 GeV for the respective cases shown. The efficiency shown in both plots is similar above 300 GeV and is much higher below 100 GeV for the time image cleaning as lower cleaning levels have been used.

3.3.2 Cut Efficiencies

The efficiency of the applied cuts for two different image cleaning methods is shown in Figure 10. It is clearly seen that the time image cleaning achieves a higher cut efficiency at energies around and below 100 GeV. Cut efficiencies are similar from $\sim$ 150 GeV onwards.

3.3.3 Spectrum, Unfolding and Spectral Energy Density Plots

Since the measured distribution of a quantity (here in our case, the spectrum of Crab) is a convolution of the *true distribution* with the response function of the telescope, one has to invert the convolution which is called 'unfolding'. We used the classes of unfolding available in the standard analysis chain of MAGIC where the distribution of excess events in terms of estimated energy, as determined by the *flux* macro, is converted to a distribution of excess events in *true energy*. We used three different unfolding methods (Bertero, Thikonov and a forward unfolding).

The overlaid spectral energy distributions of all computed spectra is shown in Figure 11. The range in which the spectral points move indicate systematics that originate from differences in the different analyses. In addition, one should keep in mind that in reality statistical fluctuations also contribute to the shifts of the spectral points especially at lower energies. At lower energies there two obvious

[2]by data sets we mean 3 sets of standard image cleaning and three of time image cleaning

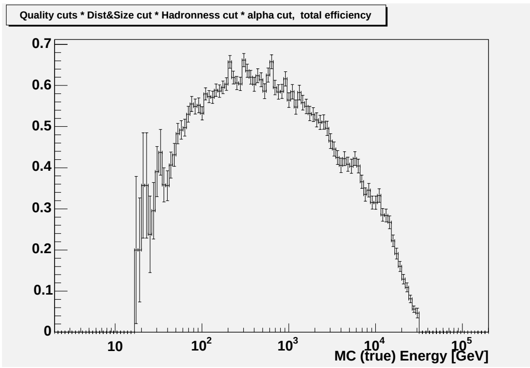

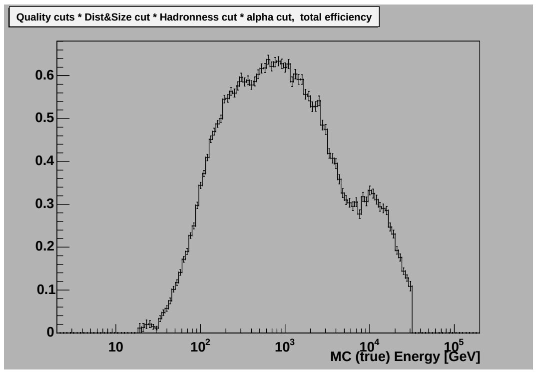

Figure 10: **Left Panel:** Cut efficiencies for one of the compiled spectra. Image cleaning 5 and 3 absolute has been applied. Alpha and Hadronness Cuts have been derived from Monte Carlo for a fixed gamma efficiency of 80%. The efficiency of the dist cut was set to retain 90% of all Gammas. **Right Panel:** Cut efficiencies for one of the compiled spectra after an image cleaning of 10 and 5 absolute has been applied. Dist, Alpha and Hadronness Cuts have been derived from Monte Carlo for fixed gamma efficiencies as outlined in the text.

reasons for systematic shifts of the spectral points:

- Little or no suppression of background events which enhances the impact of small changes in the (daily) performance of the telescope.
- Miss match between data and MC e.g. different trigger thresholds, trigger efficiencies, ...

Inhomogeneities in the acceptance of the camera are another systematic effect that is contributing to an underestimation of the flux. This effect is most important for the lowest energies. From the distribution of the center of gravities of the events ($<$ 200phe) within the camera we estimate the impact of the inhomogeneities on the calculation of the flux to be between 10% and 20% below 100 GeV. This estimate is not taking possible effects into account that contribute to a global shift in the trigger efficiency and which are not simulated in the Monte Carlo.

As will be shown in the next section, the spectrum at higher energies is on average below the published values. We found that by applying looser hadronness cuts, than those derived automatically, the spectral points move up and are in agreement with the published ones. One reason for this behavior is that by applying loose cuts one becomes less dependent on MC which is compensating some of the deficiencies between data and MC at these energies.

3.3.4 Comparison with other Experiments

We compare our results with other experiments taking a typical spectrum each from standard and time image cleaning methods. Figures 12 and the left panel in Figure **??** show the synchrotron and the Inverse Compton spectra for the Crab for two cases. The range of the systematic and statistical fluctuations that give rise to shifts of the spectral points is indicated by the shaded region. For the spectrum in Figure 12 a corepixel cut > 7 has been applied to match the differences in the trigger threshold between MC and Data.

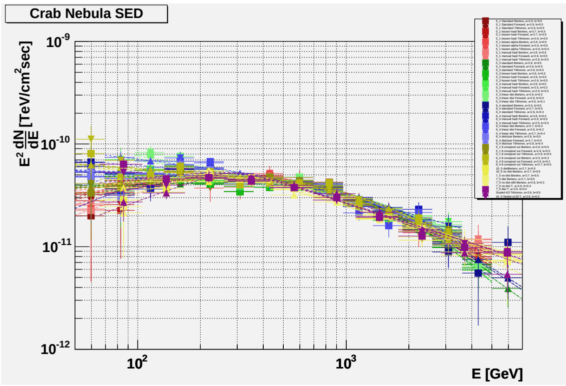

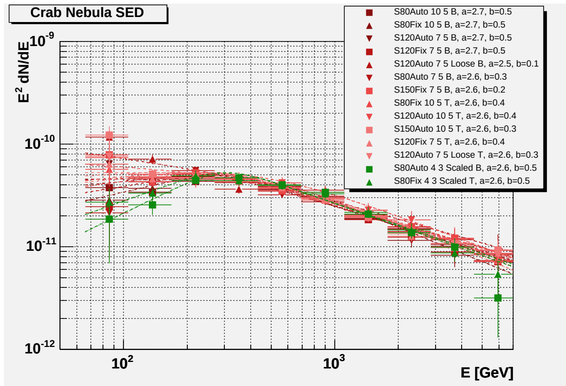

Figure 11: **Left Panel:** Spectral energy distributions (SEDs) for the data set with time image cleaning applied. **Right Panel:** SEDs for the data set processed with the standard image cleaning.

3.4 Monte Carlo Data Comparisons

In this section we show the comparisons of the Hillas parameters between the Monte Carlo gammas and the excess events obtained from the data. We apply filter cuts and a very loose cut in hadronness so as to remove the very hadron-like events from the data. The basic idea is that the differences in the distributions of Hillas parameters for ON and OFF data samples are to be exploited to extract the signal and then compare the resulting distributions with the Monte Carlo gammas. The comparisons are made in bins of size, namely, 100-200-400-600-1000-2000-5000 photoelectrons.

Figures 16, 17, 18 and 19 show the comparisons between Monte Carlo gammas and the excess events from data for the various parameters in different size-bins for image cleaning 10 5 absolute. Figures 20, 21, 22 and 23 show the same comparisons for the time image cleaning with absolute cleaning levels 6 and 4 applied.

Above 200 photoelectrons, the comparisons look reasonably OK except for the WIDTH parameter which is bad in the size bin 200-400 photoelectrons and also in the highest size bin ($>$ 2000 photoelectrons). From these studies, we conclude that the additional PSF of 14 mm used in the camera simulations reasonably describe the data except for the highest size bin. This discrepancy is not well understood and may be because of the following reasons :

- Wrongly simulated PSF (currently a single gaussian in X and Y)
- Aberrations due to frame deformation not properly simulated

For energies below 100GeV (correspondingly <200phe for the 10 5 image cleaning applied here) a MC–Data comparison is not possible. Even though the Hillas parameters for ON and OFF data match quite well in this size bin, very small differences in the image parameters are introduced due to changes in the trigger threshold, weather and NSB conditions, etc. These differences ¡¡become visible after the subtraction of ON and OFF and obscure the signal as at these energies the number of background events is much larger than the number of excess events.

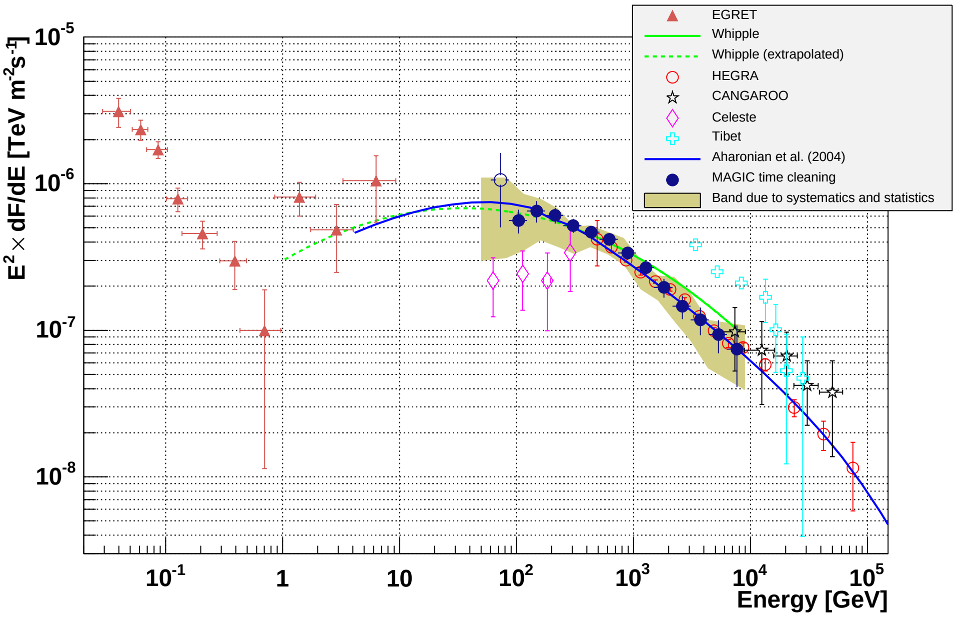

Figure 12: The shaded region gives the range in which the data points of all compiled spectra are located that are shown in Figure 11. The spectrum on top of this band has been produced with time image cleaning 6 4 absolute and loose hadronness cuts. To match the threshold in MC with the data a corepixel cut > 7 has been applied in addition.

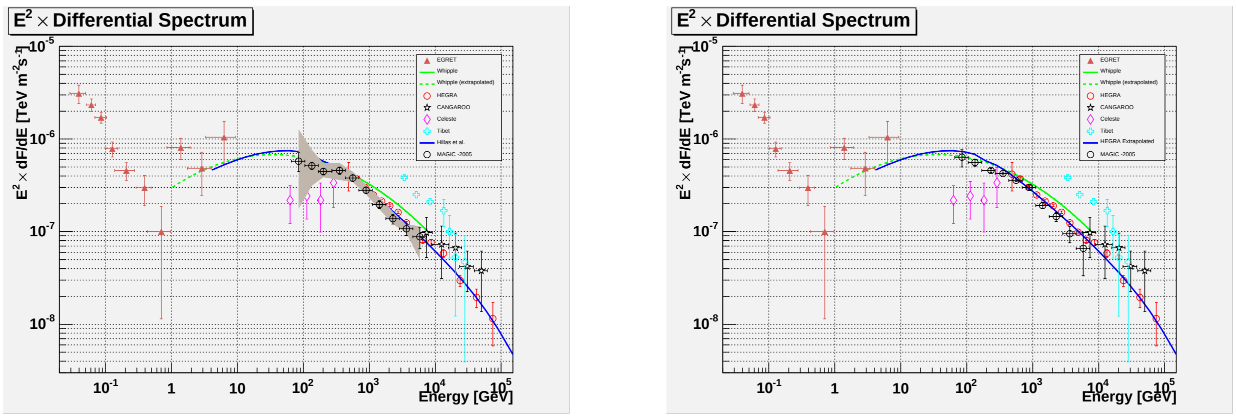

Figure 13: **Left Panel:** The grey band gives the range in which the data points of all spectra for different analysis of standard image cleaning were computed. In addtion, one typical spectrum (10/5 image cleaning) is also shown. **Right Panel:** Crab Spectral Energy Distribution for 7/5 Image cleaning method

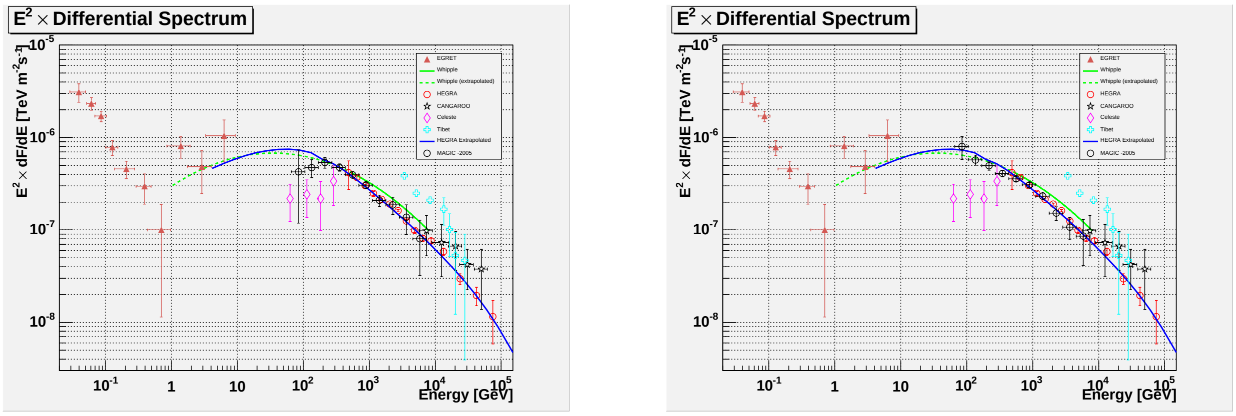

Figure 14: **Left Panel:** Spectral Energy Density Plot for Crab for 10/5 image cleaning method and loose gamma/hadron separartion cuts. **Right Panel:** Spectral Energy Density Plot for Crab for 7/5 image cleaning method and loose gamma/hadron separartion cuts. In both analysis a higher cut-efficiency is demanded

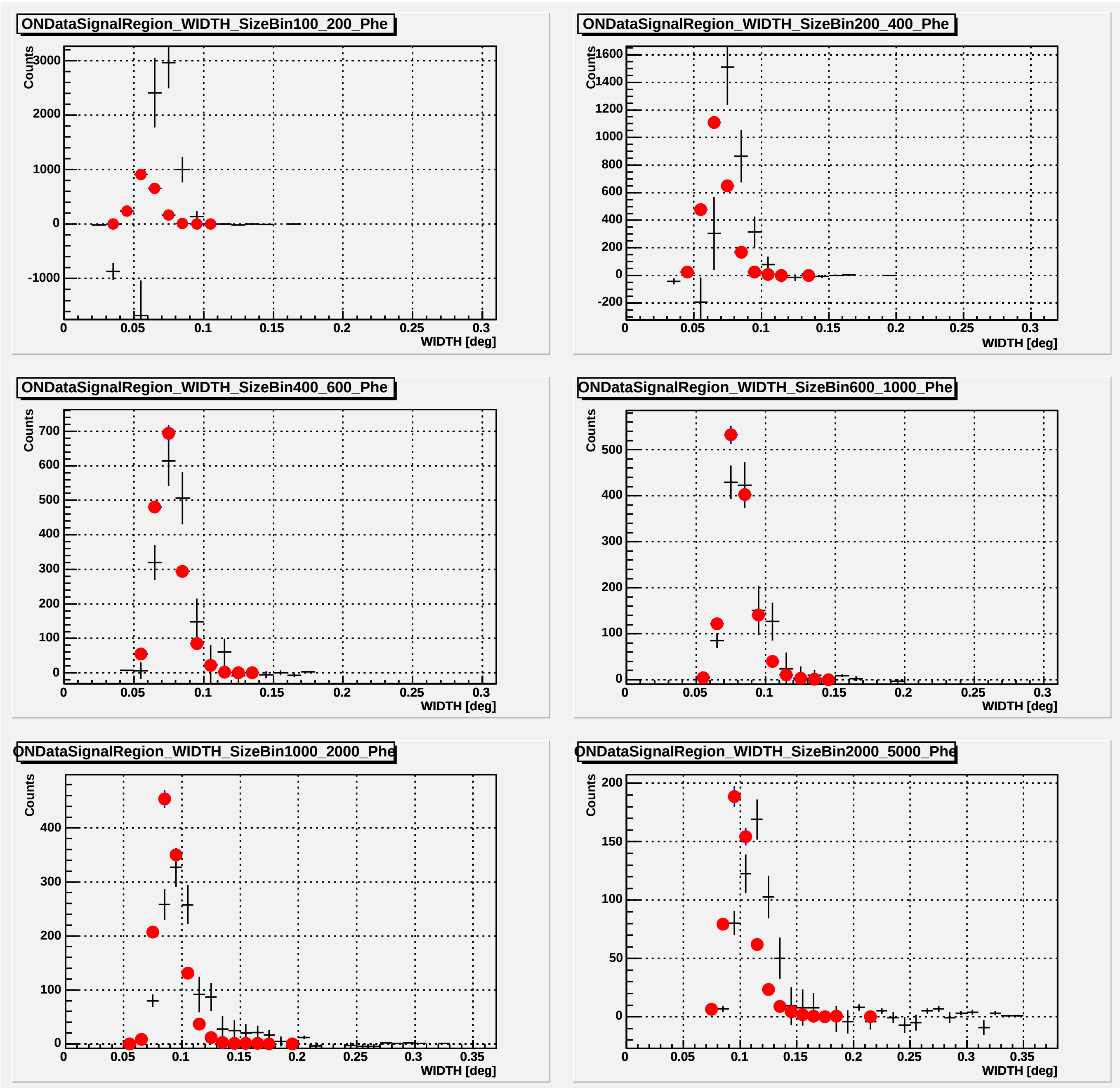

Figure 15: MC-Data Comparisons for Width parameter (10/5 cleaning). The red dots correspond to the MC γ and the black crosses correspond to the excess events (ON-OFF) from the data.

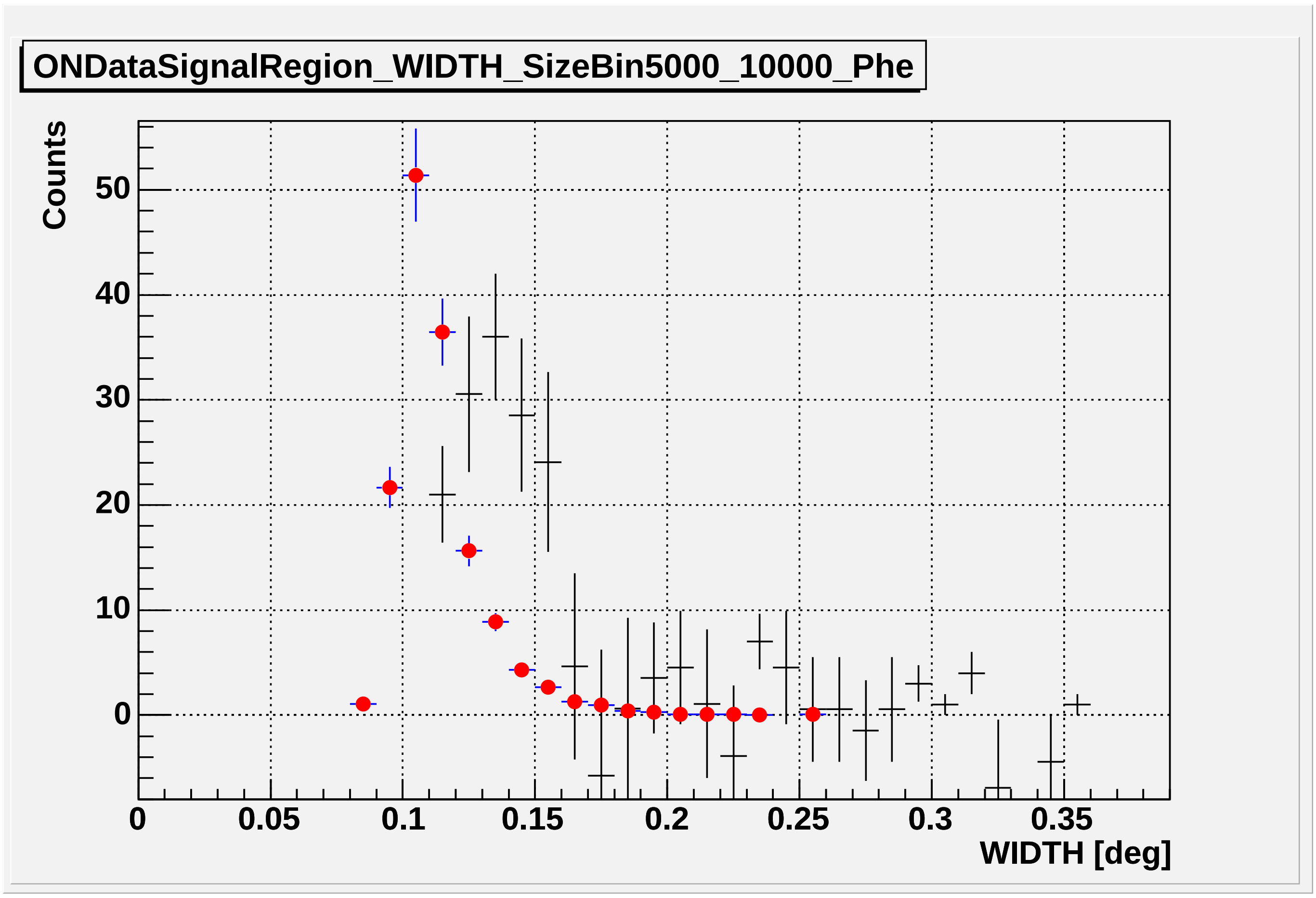

Figure 16: MC-Data Comparisons for Width parameter with a size cut > 5000 phe (10/5 cleaning). A clear miss match is visible. The red dots correspond to the MC γ and the black crosses correspond to the excess events (ON-OFF) from the data.

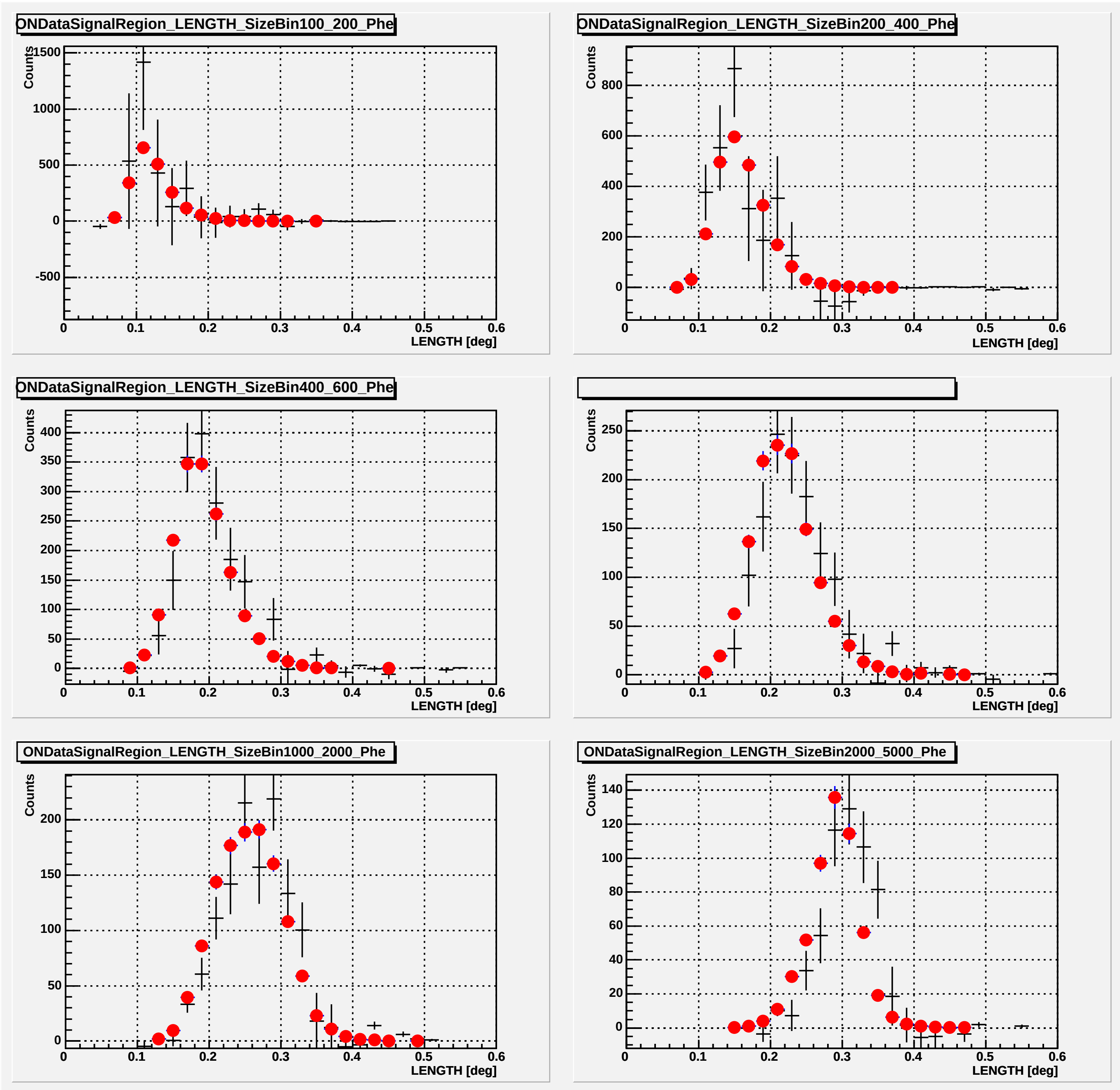

Figure 17: MC-Data Comparisons for Length parameter (10/5 cleaning). The red dots correspond to the MC γ and the black crosses correspond to the excess events (ON-OFF) from the data.

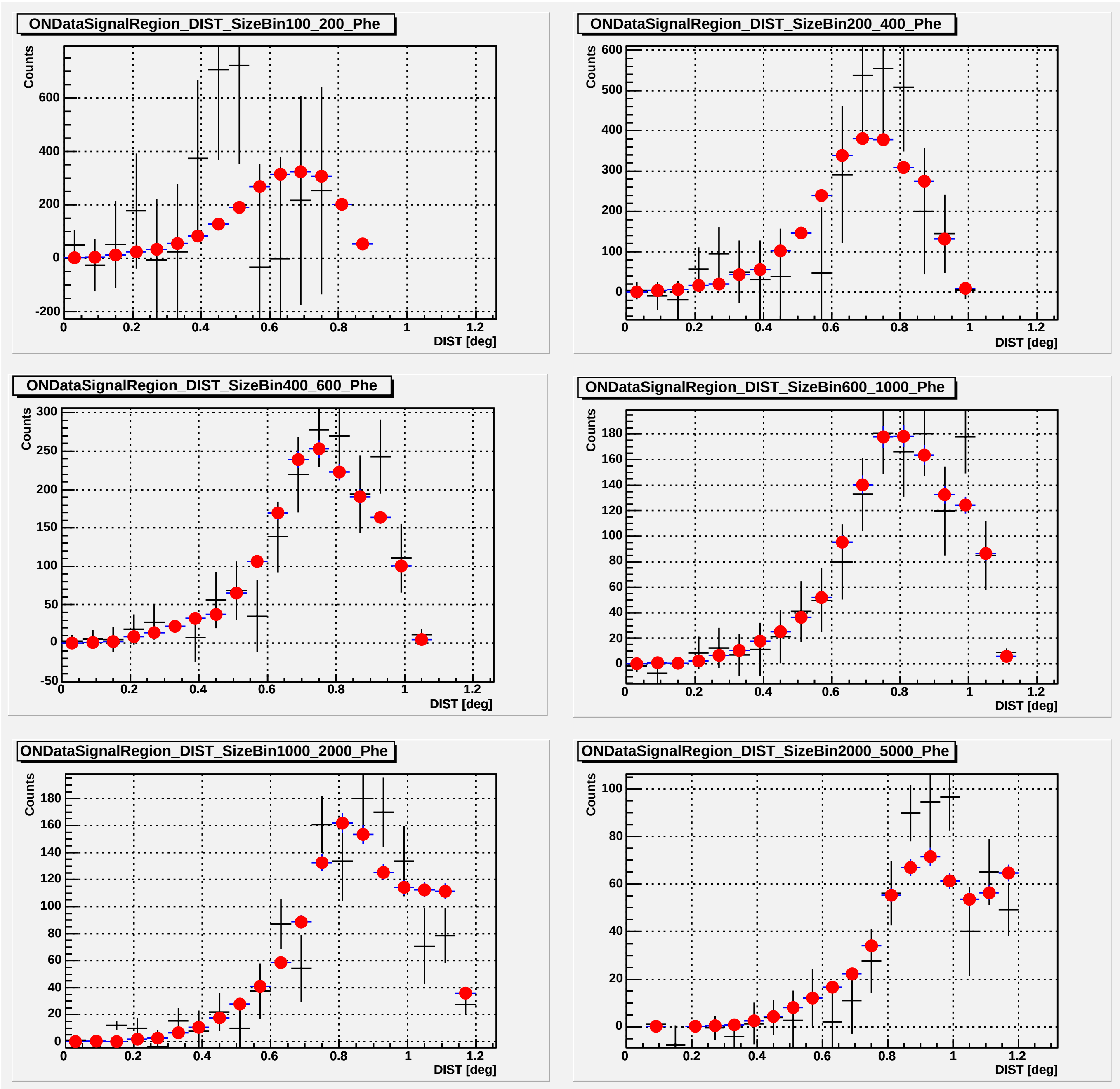

Figure 18: MC-Data Comparisons for Dist parameter (10/5 cleaning). The red dots correspond to the MC γ and the black crosses correspond to the excess events (ON-OFF) from the data.

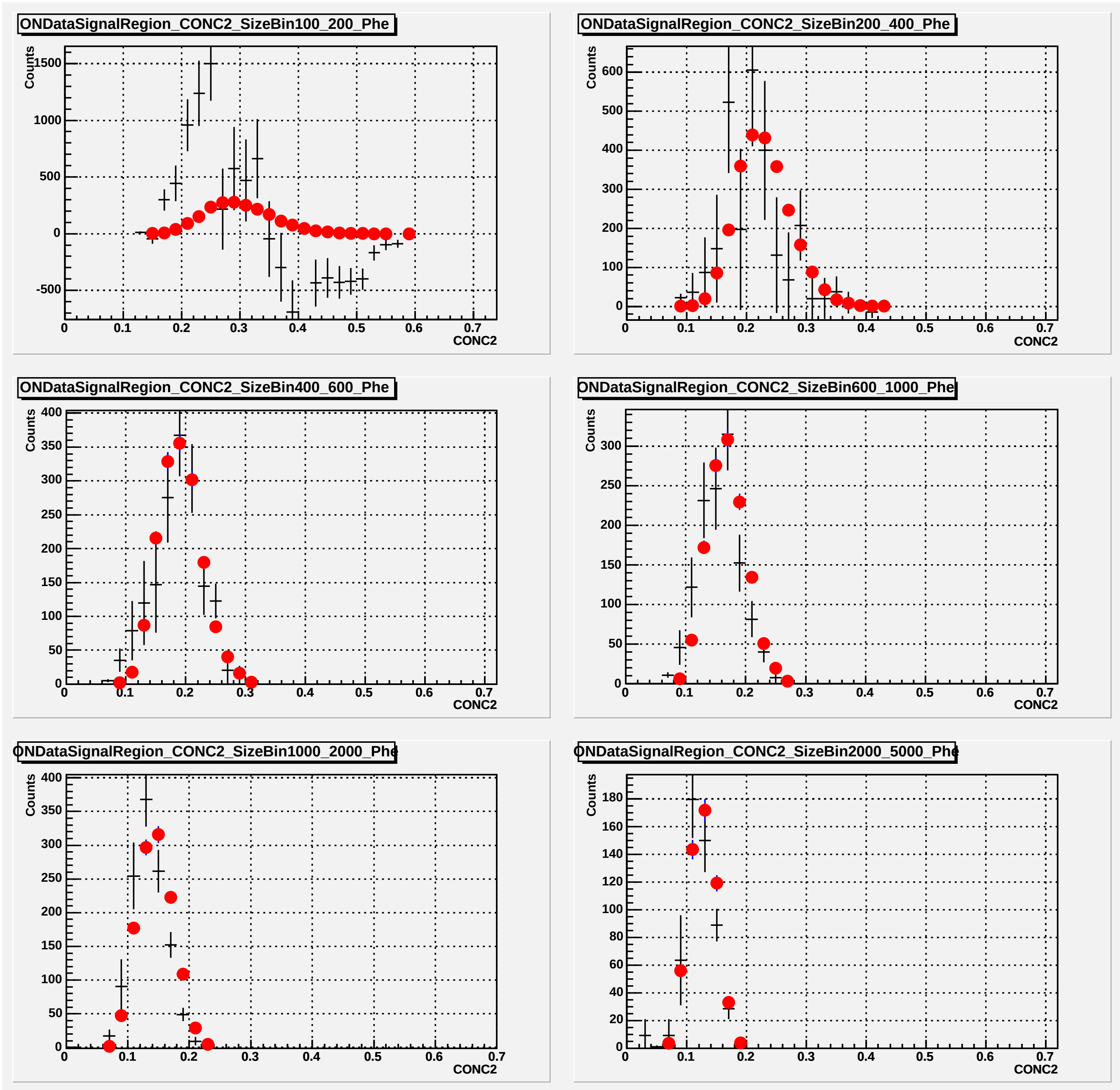

Figure 19: MC-Data Comparisons for Concentration parameter (10/5 cleaning). The red dots correspond to the MC γ and the black crosses correspond to the excess events (ON-OFF) from the data.

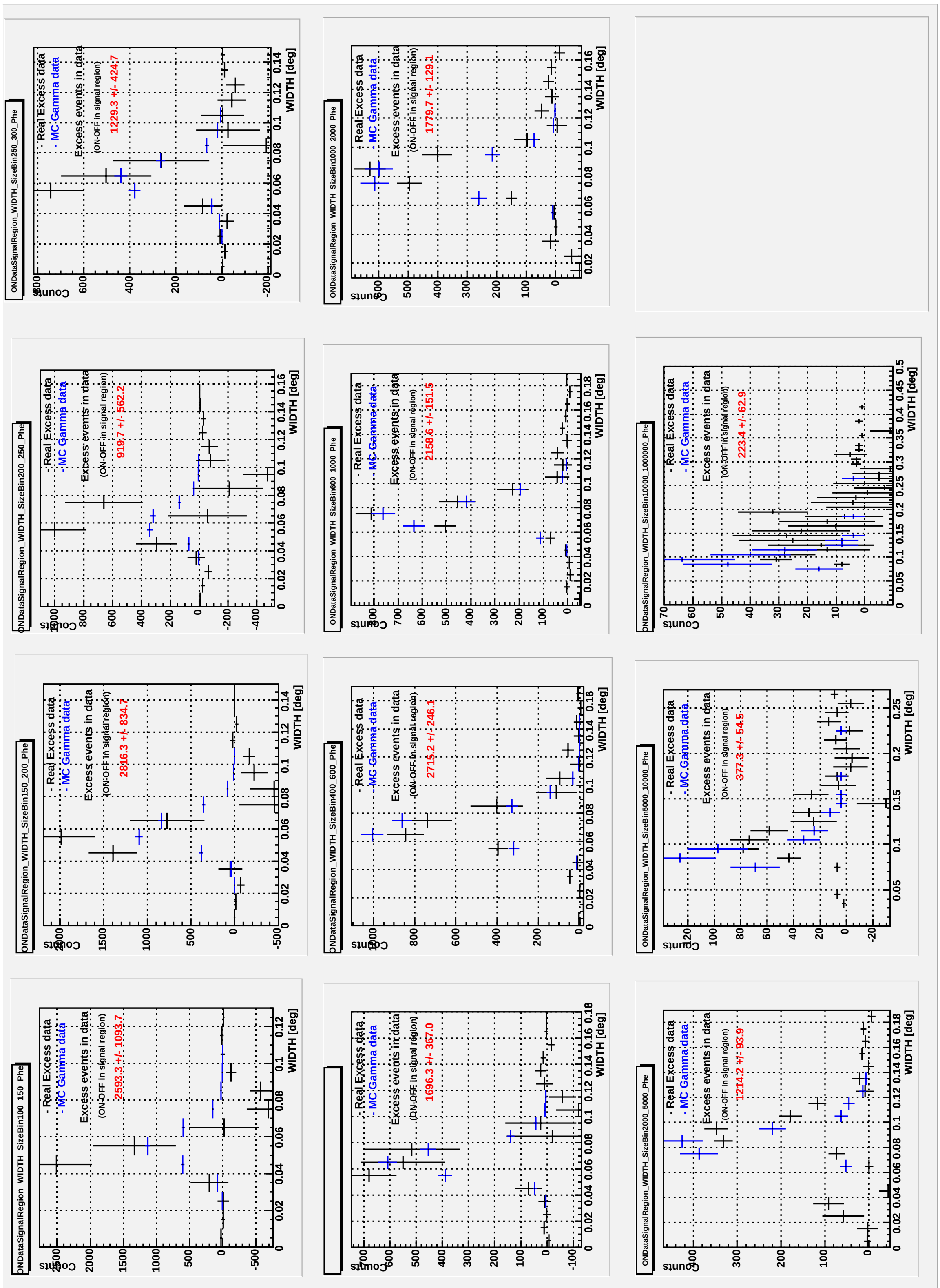

Figure 20: MC-Data Comparisons for Width parameter (6/4 cleaning)

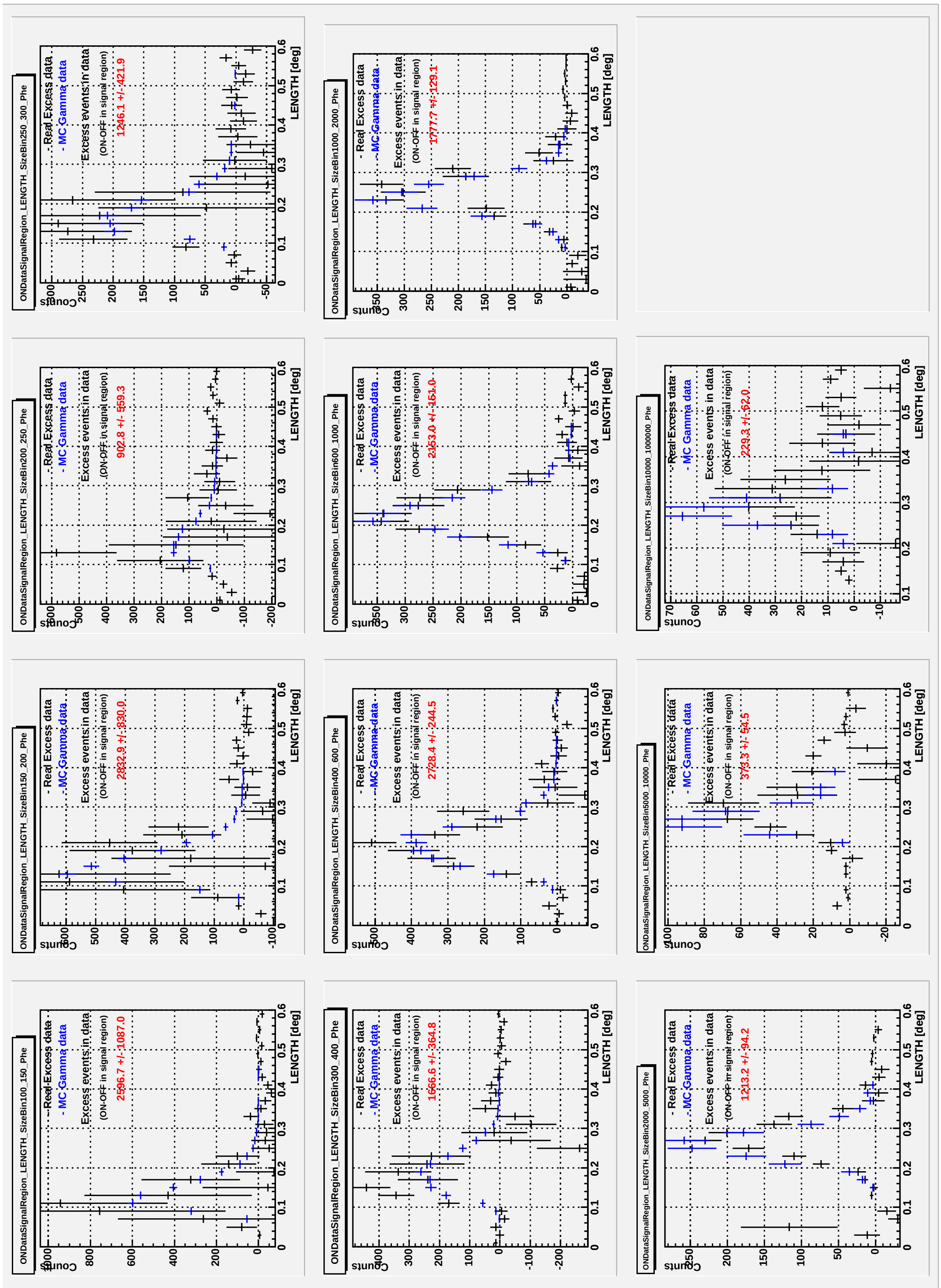

Figure 21: MC-Data Comparisons for Length parameter (6/4 cleaning)

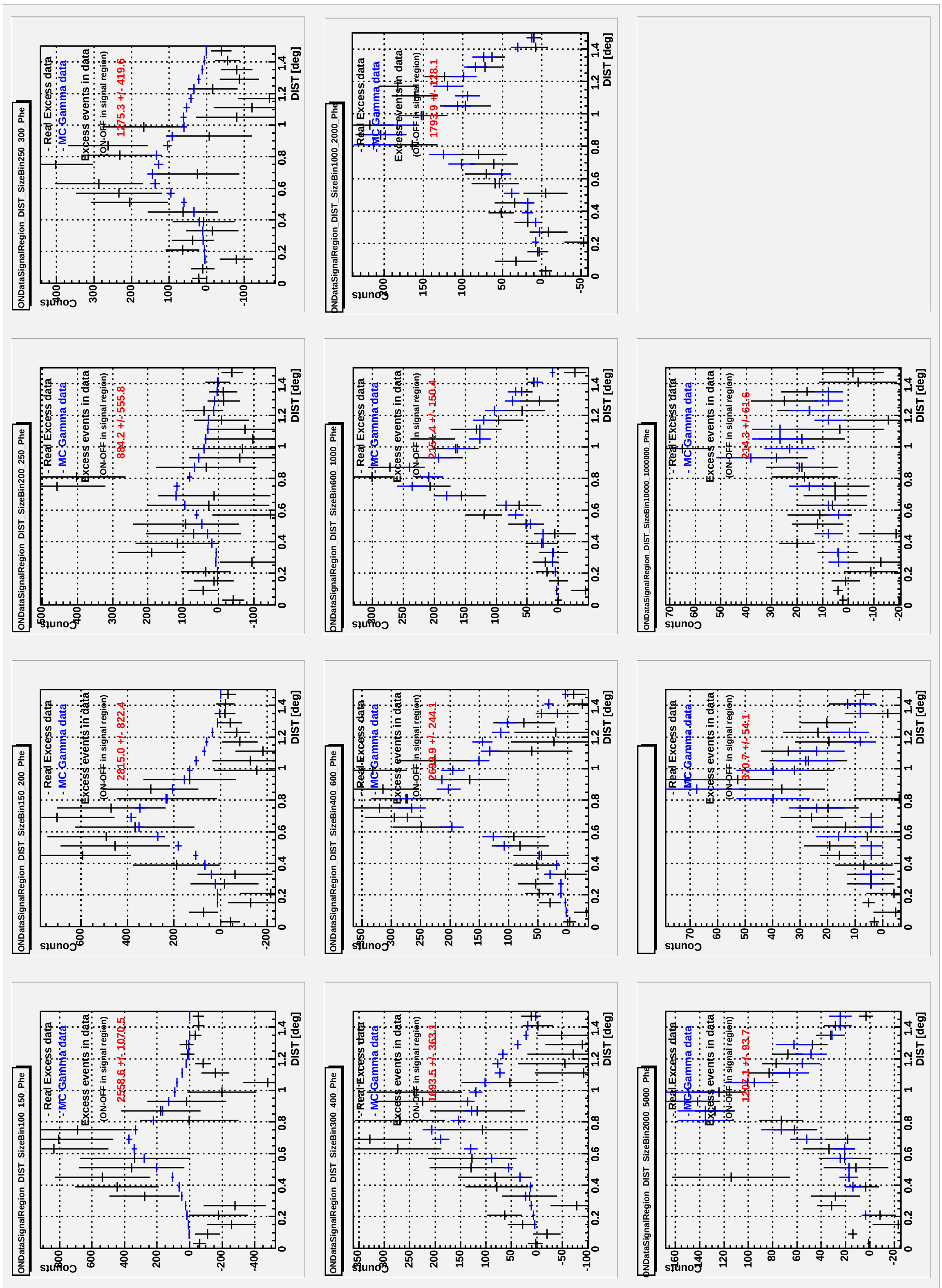

Figure 22: MC-Data Comparisons for Dist parameter (6/4 cleaning)

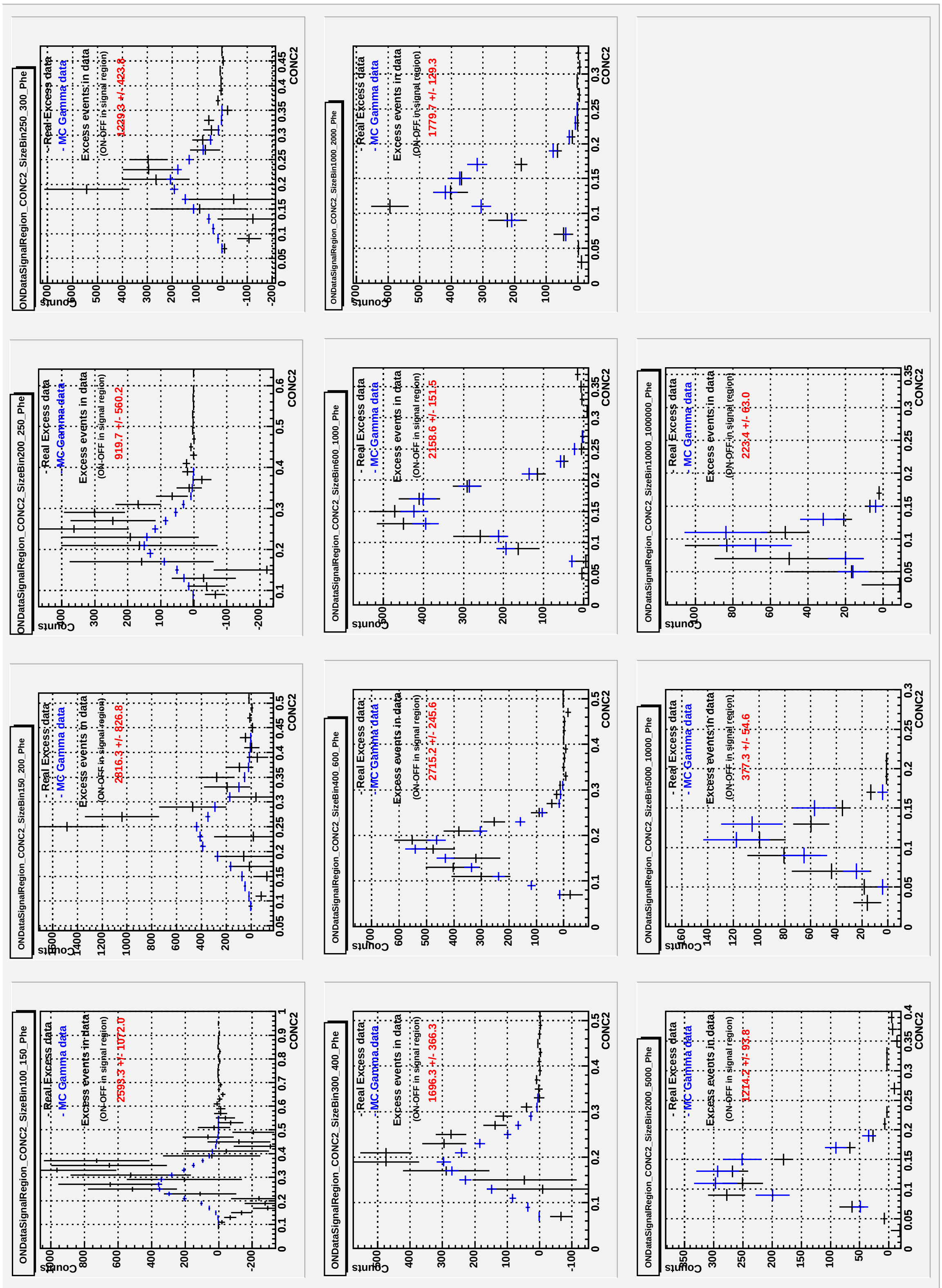

Figure 23: MC-Data Comparisons for Conc2 parameter (6/4 cleaning)

4 Discussion

We have made a detailed analysis of the data collected on Crab in 2005. The sensitivity that we calculated is on average in agreement with Monte Carlo predictions. The 1 σ confidence interval of the day to day fluctuations is 7% and therefore larger than the 5% that are expected only from statistics.

Different image cleaning methods (both 'time' and 'standard') and different analysis cuts have been used to compute the spectra in order to estimate the systematics of the analysis. We can clearly conclude that *time image cleaning method* can lower the analysis threshold of the experiment[3].

When applying cuts derived from Monte Carlo the flux points significantly deviate from the expected values for energies above one TeV. Although difficult to quantify the deviations from the expected values seem to be larger for image cleanings in which lower cleaning levels are applied (s. Figure 13). The deviations become less or vanish if looser cuts in hadronness are applied. This behavior is independent of the image cleaning which has been used to process the data as can be seen in Figure 14.

From the comparison of the Data with Monte Carlo we conclude that a miss match in the image parameter "width" and not so pronounced in other image parameters is most likely the reason for a wrong estimation of cut efficiency and subsequently responsible for the shift of the spectral points to lower values.

In order to support this argument, we analysed the data using very loose hadronness cuts in order to keep the cut-efficiencies > 60% in a wide energy band from 150 GeV to a few TeV. We see that in the case of 7/5 cleaning, the flux points above a 1 TeV seem to systematically shift upwards matching the published data for the case when high cut-efficiency is demanded (refer to the right panel in Figure 14) This effect is not so evident in case of 10/5 image cleaning method.

The systematics of the analysis are quite high below 100 GeV as is seen from Figures 12 and the left panel in Figure 13 pointing to the fact that the analysis methods fail to reduce the background. This can also be seen from the differential sensitivity which is gradually worsening when going to lower energies (s. Table 3). It should be noted that this does not include the systematics of the instrument. However, the systematics for the *time image cleaning* analysis is seen to be lower than the *standard image cleaning* analysis for the same energy (at 80 GeV) because the cut efficiency at energies below 100 GeV is higher for the time image cleaning. The reason is that the additional constraint in time that is used in the time image cleaning allows to lower the cleaning levels without picking up too much noise. As a result more events which can be analyzed are accepted on the level of image cleaning which are lost when one uses higher cleaning levels. Another contribution to the systematics in the analysis arises from differences between Monte Carlo and data, near the trigger threshold. These differences lead to wrong cut efficiencies. We observed that the flux points below 100 GeV systematically move up if one raises the *minimum size cut* and the *corepixel cut* in the analysis (as mentioned before).

[3]it is $\sim$ 60 GeV for *time image cleaning method* and $\sim$ 80 GeV for *standard image analysis*